

Energy Gap-Refractive Index Relations in Semiconductors – Using Wemple-DiDomenico model to unify Moss, Ravindra, and Herve-Vandamme Relationships

[Aneer Lamichhane](#) *

Posted Date: 11 August 2023

doi: 10.20944/preprints202308.0861.v1

Keywords: energy gap; refractive index; Moss, Ravindra, Herve-Vandamme relationships; Wemple and DiDomenico single oscillator model




Preprints.org is a free multidiscipline platform providing preprint service that is dedicated to making early versions of research outputs permanently available and citable. Preprints posted at Preprints.org appear in Web of Science, Crossref, Google Scholar, Scilit, Europe PMC.

Copyright: This is an open access article distributed under the Creative Commons Attribution License which permits unrestricted use, distribution, and reproduction in any medium, provided the original work is properly cited.

Article

Energy Gap-Refractive Index Relations in Semiconductors—Using Wemple-DiDomenico model to Unify Moss, Ravindra, and Herve-Vandamme Relationships

Aneer Lamichhane 

Western Colorado University, Department of Natural and Environmental Sciences, Hurst Hall 110, Gunnison, 81231, CO, United States; Aneer.Lamichhane@njit.edu/alamichhane@western.edu; Tel.: 720-755-1345

Abstract: The refractive index of solids gauges their transparency to incident light, while the energy gap determines the threshold for light absorption. This paper provides a mathematical formulation for the relationship between refractive index and energy gap. It is also established that this formulation aided in the unification of the Moss, Ravindra, and Herve-Vandamme relationships.

Keywords: energy gap; refractive index; Moss, Ravindra, Herve-Vandamme relationships; Wemple and DiDomenico single oscillator model

1. Introduction

Light interacts with solids through several ways, depending on the material and incident frequency under consideration. Many semiconductors are normally opaque to some higher frequencies and transparent to lower frequencies. Insulators or dielectrics are mostly transparent to visible light and metallic solids appear shiny as they reflect practically any frequency of light. The complex refractive index is adequate to assess light interaction with solids. Depending on the frequency of incident light, a material with a real refractive index closer to unity is generally transparent to that incident light, and transparency decreases with increasing refractive index. The energy gap, on the other hand, defines the threshold for light absorption in solids. In semiconductors, opacity is defined by incident photon energy surpassing the energy gap. Visible light is not absorbed by insulators or dielectrics due to their wider energy gap. Because metallic solids lack an energy gap, mobile electrons reflect incident photons, making them shine. As a result, one can simply conclude that the refractive index has an inverse relationship with the energy gap. Furthermore, the refractive index and the energy gap are two fundamental variables that play an important role in understanding electronic, optical, or optoelectronic properties in semiconductor based devices [1–3]. In general, a material's refractive index is a function of frequency and doping, and various literature studies highlight the refractive index's dependence on thickness, voids, grain boundaries, and other parameters [4–6]. To avoid such variations, it is best practice to consider the static refractive index determined from the time-independent electric field, and it should be noted that this article only addresses the static refractive index.

In 1950, Moss was the first to establish the inverse relationship between refractive index (n) and energy gap (E_g) [7]. This relationship was built on the broad assumption that all energy levels in a solid are scaled down by a factor of $\frac{1}{\epsilon_{eff}^2}$, where ϵ_{eff} being the effective dielectric constant ($\epsilon_{eff} \approx n^2$). The photo effect process that occurs in the lattice defects found in alkali halides provides support for this claim. Such lattice defect spots behave as hydrogen-like centers where the electron behaves as an electron in an isolated atom with a bulk material-based dielectric constant. As a result, there appears to be some correlation between the scale factor and the ionization energy of the hydrogen atom. Moss observed a good relationship between the experimental data of the threshold long wavelength λ for

photoconductive substances with the corresponding refractive index n and found that the ratio $\frac{n^4}{\lambda}$ close to $77 / \mu m$. Regarding the energy gap, the Moss relation becomes

$$n^4 E_g = 95 \text{ eV} \quad (1)$$

The constant on the right hand side of Equation 6 is found by fitting the data and depends on the solids' lattice structure. One of the limitations of the Moss relation is the lack of uniqueness of its constant. According to Moss, the constant for zinc blende and diamond structure lies within $\pm 8\%$ of 174 eV [8]. Based on the nature of the constant, numerous adjustments to the Moss relation are made by better fitting experimental data. Ravindra and Srivastava [9] proposed the following revised value of Moss constant,

$$n^4 E_g = 108 \text{ eV} \quad (2)$$

Similarly, Reddy and Ahammed [10] altered Moss's relationship as

$$n^4 (E_g - 0.365) = 154 \text{ eV} \quad (3)$$

Since the energy levels in a solid are highly complex and require band structure theory, all of these variations are caused by a structural restriction on the Moss relation. Second, the constant can vary amongst solids, ranging from direct to indirect interband transitions.

In 1979, Ravindra et al. [11] proposed an alternative linear empirical relation linking n with E_g as,

$$n = K_1 - K_2 E_g \quad (4)$$

where the values of the constants K_1 and K_2 , which were determined through empirical fitting, are 4.084 and 0.62 eV^{-1} , respectively. After a year, the mathematical underpinnings of this linear relation were provided by Gupta and Ravindra [12], based on the Penn model [13] and Wemple-DiDomenico single oscillator model [14,15]. Their formulations made the assumption that the trajectories of the valence and conduction bands are roughly parallel to one another, at least along the symmetry axes, and that the difference between the Penn gap or the oscillatory resonance energy with the energy gap is constant. In contrast to the Moss relation, the Ravindra relation has no structural constraints. The latter relation, on the other hand, places an upper limit on the refractive index (do not predict refractive index beyond 4.1) and provides a good approximation for the intermediate value of the energy gap (from 0.3 eV to 3.5 eV) in semiconductors. One serious limitation of Ravindra relation is that it gives negative indices for $E_g > 6.6 \text{ eV}$.

In 1994, Herve and Vandamme [16] presented n - E_g relationship based on the classical oscillatory theory as

$$n = \sqrt{1 + \left(\frac{A}{E_g + B}\right)^2} \quad (5)$$

where A and B are constants. The value of B is thought to reflect a constant difference between the UV resonance energy and the energy gap, which is 3.4 eV , whereas the constant A was discovered by fitting to be 13.6 eV , which corresponds to the hydrogen ionization energy. Except for $IV - VI$ materials (PbS , $PbSe$, $PbTe$), the Herve-Vandamme relation provides a good fit to the related experimental data for the majority of materials.

Since 1950, multiple empirical relations have been proposed by various researchers to account for both the structural and refractive index restrictions of the Moss and Ravindra relations. There is still a lack of a robust theoretical foundation in this discipline. Finkenrath [17] used the band theory in 1988 to theoretically develop the Moss-like relation ($(\epsilon_{eff} - 1)^2 E_g = \text{constant}$) and the Ravindra relation.

This paper's main goal is to establish a single mathematical framework for the formulation of Moss, Ravindra, and Herve-Vandamme relationships. Since these relationships are empirical, the

physical knowledge of the fitting parameters (constants) is limited. Additionally, this work aims to provide light on these fitting parameters.

2. Mathematical formulation

This model suggests an arbitrary function $f(E_g)$, which is expressed as a power series of E_g as,

$$f(E_g) = \sum_{n=0}^{\infty} (-1)^n K_n E_g^{np} = K_0 + \sum_{n=1}^{\infty} (-1)^n K_n E_g^{np} \quad (6)$$

where, p is a number and it will be shown here that for a suitable value of p , the series (6) converges to

$$K_0 \left[1 + \frac{E_g^p}{K^p} \right]^{-1/p} \quad (7)$$

iff

$$K_n = \frac{K_0}{n! p^n K^{np}} \prod_{i=1}^n [1 + (i-1)p], \forall n \in I \text{ \& } n \geq 1 \quad (8)$$

Proof. Starting from

$$f(E_g) = K_0 + \sum_{n=1}^{\infty} (-1)^n K_n E_g^{np} \quad (9)$$

and substituting the value of K_n from equation (8) yields,

$$f(E_g) = K_0 \left[1 + \sum_{n=1}^{\infty} \left\{ \frac{(-1)^n}{n! p^n} \left(\frac{E_g}{K} \right)^{np} \prod_{i=1}^n [1 + (i-1)p] \right\} \right] \quad (10)$$

evaluating the summation and rearranging yields,

$$\begin{aligned} f(E_g) = & K_0 \left[1 + \left(-\frac{1}{p} \right) \left(\frac{E_g^p}{K^p} \right) + \frac{1}{2!} \left(-\frac{1}{p} \right) \left(-\frac{1}{p} - 1 \right) \left(\frac{E_g^p}{K^p} \right)^2 + \right. \\ & \frac{1}{3!} \left(-\frac{1}{p} \right) \left(-\frac{1}{p} - 1 \right) \left(-\frac{1}{p} - 2 \right) \left(\frac{E_g^p}{K^p} \right)^3 + \frac{1}{4!} \left(-\frac{1}{p} \right) \left(-\frac{1}{p} - 1 \right) \\ & \left. \left(-\frac{1}{p} - 2 \right) \left(-\frac{1}{p} - 3 \right) \left(\frac{E_g^p}{K^p} \right)^4 + \dots \right] \quad (11) \end{aligned}$$

The bracketed terms is a well-known binomial series, which converges to an equation (7) whenever $\left| \frac{E_g^p}{K^p} \right| < 1$

$$f(E_g) = K_0 \left[1 + \frac{E_g^p}{K^p} \right]^{-\frac{1}{p}} \quad (12)$$

Conversely, let us define a function

$$g\left(\frac{E_g^p}{K^p}\right) = \left[1 + \frac{E_g^p}{K^p} \right]^{-\frac{1}{p}} \quad (13)$$

then, the value of g and its derivatives at zero can be found as,

$$g(0) = 1 \quad (14)$$

$$g^{(i)}(0) = -\frac{1}{p} \quad (15)$$

$$g^{(ii)}(0) = \left(-\frac{1}{p}\right)\left(-\frac{1}{p} - 1\right) \quad (16)$$

$$g^{(iii)}(0) = \left(-\frac{1}{p}\right)\left(-\frac{1}{p} - 1\right)\left(-\frac{1}{p} - 2\right) \quad (17)$$

$$g^{(iv)}(0) = \left(-\frac{1}{p}\right)\left(-\frac{1}{p} - 1\right)\left(-\frac{1}{p} - 2\right)\left(-\frac{1}{p} - 3\right) \quad (18)$$

$$\dots\dots\dots \quad (19)$$

$$g^{(n)}(0) = \frac{1}{p^n} \prod_{i=1}^n [1 + (i-1)p] \quad (20)$$

This allows to express $g(\frac{E_g^p}{K^p})$ and $f(E_g)$ as,

$$g(\frac{E_g^p}{K^p}) = \sum_{n=0}^{\infty} \frac{g^{(n)}(0)}{n!} \left(\frac{E_g^p}{K^p}\right)^n \quad (21)$$

$$f(E_g) = K_o \sum_{n=0}^{\infty} \frac{g^{(n)}(0)}{n!} \left(\frac{E_g^p}{K^p}\right)^n \quad (22)$$

Comparing equation (22) with equation (6) yields,

$$K_n = \frac{K_o}{n! p^n K^{np}} \prod_{i=1}^n [1 + (i-1)p] \quad (23)$$

Furthermore, the convergence condition $|\frac{E_g^p}{K^p}| < 1$ yields the following two possibilities:

- (i) positive p and $K > E_g \Rightarrow |\frac{E_g^p}{K^p}| < 1$
- (ii) negative p and $E_g > K \Rightarrow |\frac{E_g^p}{K^p}| < 1$

This completes the proof. Here, it is not disclosed about K_o and K . In the next section, the search for the physical meaning of K_o , K and p is implemented. \square

3. K_o , K and p

The well-known Sellmeier dispersion model [18] is,

$$n^2 - 1 = \sum_i A_i \quad (24)$$

A_i is the empirical parameter that corresponds to the strength of undamped Lorentz oscillators. Using generalized Lorentz oscillator model [19],

$$n^2 - 1 = \omega_p^2 \sum_i \frac{f_i}{\omega_i^2} \quad (25)$$

where ω_p is the plasma frequency and f_i is the oscillator strength associated with transitions at frequency ω_i . Wemple and DiDomenico (WD) [14,15] suggested a single oscillator model that could be considered dominant among other oscillators and proposed,

$$n^2 - 1 = \frac{F}{E_o^2} \quad (26)$$

F being the overall oscillator strength and is given as,

$$F = \hbar^2 \omega_p^2 \sum_i \frac{\omega_j^2}{\omega_i^2} f_i \quad (27)$$

ω_j is the dominant oscillator frequency. Using the r^{th} moment of the optical spectra and Kramers-Kronig relation [14,15], WD found that $F = E_o E_d$, where the parameters E_o and E_d are the oscillator resonance energy and dispersion energy, respectively. In terms of Sellmeier model this can also be written for j^{th} dominant oscillator as $A_j = \frac{E_d}{E_o}$, where A_j is the dominant oscillatory strength instead of the electric-dipole oscillator strength associated with transitions at a specific frequency. Thus, the well known WD model is,

$$n^2 = 1 + \frac{E_d}{E_o} \quad (28)$$

If K is the separation of the dominant oscillator energy E_o from the minimum energy gap E_g then under the condition $K > E_g$ the WD model can be written as,

$$n^2 = \frac{E_o + E_d}{K} \left[1 - \left(\frac{E_g}{K}\right) + \left(\frac{E_g}{K}\right)^2 - \left(\frac{E_g}{K}\right)^3 + \dots \right] \quad (29)$$

Equation (29) satisfies the requirement shown by Equation (8), and therefore enables us to compare with Equation (11), which yields, $p = 1$

$$K_o = \frac{E_o + E_d}{K} \quad (30)$$

where,

$$K = E_o - E_g \quad (31)$$

Hence, the required model for the refractive index n can be written as,

$$n^2 = \sum_{n=0}^{\infty} (-1)^n K_n E_g^n = K_o + \sum_{n=1}^{\infty} (-1)^n K_n E_g^n \quad (32)$$

and based on the convergence condition (i),

$$n^2 = K_o \left[1 + \frac{E_g}{K} \right]^{-1} \quad (33)$$

In most semiconductors, the refractive index's dependence on the energy gap is mostly governed by UV oscillator energy and thus it is plausible to consider K usually exceeds E_g . Furthermore, if $p > 0$ then K might be expressed as $K = (E_o^p - E_g^p)^{1/p}$ and thus, from the band structure point of view p as unity is more preferable at least for direct band gap materials, which has also been justified by the WD model. Moreover, one can clearly notice that K_o is a unitless quantity and K has a unit of energy. In the next section, it will be shown that Equation (33) is the basis equation that can connect the Moss, Ravindra, and Herve-Vandamme relations and offer insight on the physical understanding of the constants used in these relations.

4. Results

4.1. Moss Relation

By squaring Equation (33) and simplifying one can easily get that,

$$n^4 E_g = \frac{K_o^2 K}{2 + \frac{E_g}{K} + \frac{K}{E_g}} \tag{34}$$

One can estimate Moss constant from the WD’s constant-conductivity dielectric model [14,15], which approximate the ratio E_o to E_g as,

$$\frac{E_o}{E_g} = \sqrt{\frac{3b^2}{b^2 + b + 1}} \tag{35}$$

where b is a coefficient with a value of 3.4 for covalent solids and 2.1 for ionic solids. Equation (35) allows us to write,

$$2 + \frac{E_g}{K} + \frac{K}{E_g} = \frac{3b^2}{\sqrt{3b^2} \sqrt{b^2 + b + 1} - (b^2 + b + 1)} \tag{36}$$

The term $\left[\frac{\sqrt{3b^2} \sqrt{b^2 + b + 1} - (b^2 + b + 1)}{3b^2} \right]$, therefore, has a value 0.217 for covalent solids and 0.185 for ionic solids. This suggests to write the Moss relation as,

$$n^4 E_g = [0.185, 0.217] \times K_o^2 K \approx 0.2 \times K_o^2 K \tag{37}$$

The WD’s constant-conductivity dielectric model assumes the ratio $\frac{E_o}{E_g} = 0.8\sqrt{b} \approx 1.33$, and in many solids, this ratio roughly ranges from 1.7 to 2.0, which might cause slight changes in the Moss constant. Table 1 highlights the calculated values of Moss constant for different materials.

Table 1. The data in columns 3, and 4 are from sources [14,15] and rest are calculated. Columns 5, 6, and 7 show the computed Ravindra, Herve-Vandamme, and Moss constants, respectively. The data in the second and last columns are taken from source [20].

	$E_g(eV)$	$E_o(eV)$	$E_d(eV)$	Ravindra Constants: $K_1; K_2$	H – V Constants: $A; B$	Moss Constant	$n(exp)$
C	5.4	10.9	49.7	3.32; 0.30	23.27; 5.5	166.91	2.35
Si	1.1	4.0	44.4	4.08;0.70	13.32;2.9	161.06	3.46
Ge	0.67	2.7	41.0	4.64;1.14	10.52;2.03	175.51	4.0
GaAs	1.43	3.55	33.5	4.18;0.98	10.90;2.12	155.76	3.3
GaP	2.24	4.46	36.0	4.27;0.96	12.67;2.22	184.34	2.9
InSb	0.18	2.3	35.0	4.19;0.99	8.97;2.12	47.34	3.95
AlP	2.45	5.6	34.9	3.58;0.57	13.98;3.15	128.14	2.75
AlAs	2.18	4.7	33.7	3.90;0.77	12.58;2.52	145.52	3.0
LiF	12.50	17.1	14.9	2.63;0.28	15.96;4.6	43.77	1.39
NaF	10.5	15	11.3	2.42;0.27	13.01;4.5	32.28	1.33
KF	10.3	14.8	12.3	2.45;0.27	13.50;4.5	34.53	1.36
NaCl	8.9	10.3	13.6	4.13;1.47	11.83;1.40	47.92	1.54
KCl	8.5	10.5	12.3	3.38;0.84	11.96;2	40.08	1.49
RbCl	8.3	10.4	12.2	3.28;0.78	11.26;2.1	39.19	1.49
CsCl	8	10.6	14	3.97;0.59	12.18;2.60	43.09	1.61

Table 1. Cont.

KBr	7.6	9.2	12.4	3.67;1.15	10.68;1.60	41.90	1.55
RbBr	7.2	9.1	12.1	3.34;0.88	10.54;1.90	39.08	1.55
KI	6.17	7.7	12.8	3.66;1.19	9.92;1.53	43.73	1.67
RbI	5.8	7.7	12.1	3.23;0.85	9.65;1.90	38.35	1.64
CsCl	8.0	10.6	17.1	3.26;0.63	13.46;2.6	54.63	1.61
CsBr	7.0	9.4	17	3.32;0.69	12.64;2.40	55.21	1.67
CsI	6.3	7.5	15.2	4.35;1.81	10.67;1.20	57.71	1.82
TlCl	2.11	5.8	20.6	2.67;0.36	10.93;3.69	43.71	2.08
TlBr	2.68	5.3	21.7	3.21;0.61	10.72;2.62	69.55	2.25
CaF ₂	11.8	15.7	15.9	2.84;0.36	15.80;3.90	47.80	1.43
BaF ₂	10.5	13.8	15.9	3.0;0.45	14.81;3.3	48.63	1.47
AgCl	5.13	7.4	22	3.6;0.80	12.76;2.27	80.97	1.9
CuCl	3.31	7.3	18.1	2.52;0.31	11.49;3.99	40.07	2.19
ZnO	3.7	6.4	17.1	2.95;0.55	10.46;2.70	49.88	1.92
CdS	2.4	4.9	20.4	3.18;0.64	9.99;2.5	63.98	2.38
CdSe	1.74	4.0	20.6	3.29;0.73	9.08;2.26	65.81	2.49
ZnS	3.54	6.15	25.2	3.46;0.66	12.45;2.61	91.98	2.27
MgO	7.8	11.3	22.0	3.08;0.44	15.77;3.5	67.74	1.62
CaO	6.26	9.9	22.6	2.98;0.41	14.96;3.64	67.46	1.39
Al ₂ O ₃	6.96	13.4	27.5	2.52;0.195	19.19;6.44	64.84	1.63
Y ₃ Al ₅ O ₁₂	6.5	11.1	25.4	2.82;0.31	16.80;4.60	70.28	1.71
TeO ₂	3.7	6.24	23.2	3.40;0.67	12.03;2.54	82.36	2.2
SrTiO ₃	4.10	5.68	23.7	4.31;1.36	11.60;1.58	109.70	2.38
BaTiO ₃	4.12	5.57	23.3	4.46;1.54	11.40;1.45	110.68	2.4
KTaO ₃	3.70	6.50	23.7	3.28;0.58	12.41;2.8	79.87	2.2
LiTaO ₃	4.7	7.49	26.1	3.47;0.62	13.98;2.80	94.53	2.18
LiNbO ₃	4.0	6.65	25.9	3.50;0.66	13.12;2.65	95.83	2.34
TiO ₂	3.2	5.24	25.7	3.89;0.95	11.60;2.04	111.56	2.72
MgAl ₂ O ₄	7.80	12.1	23.3	2.87;0.33	16.80;4.3	66.76	1.52
CaWO ₄	4.20	9.15	23.3	2.56;0.25	14.60;4.95	52.82	1.81
ZnWO ₄	3.56	7.46	26.0	2.93;0.37	13.93;3.9	71.62	2.1
CaMoO ₄	4.50	8.26	23.0	2.88;0.38	13.78;3.76	64.45	1.90
PbMoO ₄	3.2	5.40	22.60	3.56;0.81	11.04;2.2	86.03	2.2
SrMoO ₄	4.16	8.60	21.30	2.60;0.29	13.53;4.44	50.28	1.85
SiO ₂	9.3	13.6	18.3	2.72;0.32	15.77;4.30	51.16	1.46
ZnS	3.54	6.36	26.1	3.39;0.60	12.88;2.82	92.21	2.27
ZnSe	2.58	5.54	27.0	3.31;0.56	12.23;2.96	89.0	2.43
ZnTe	2.26	4.34	27.0	3.88;0.93	10.82;2.08	117.85	2.70
CdTe	1.58	4.13	25.7	3.42;0.67	10.30;2.55	82.42	2.7
PbS	0.286	3.5	55.33	4.28;0.66	13.91;3.21	80.55	4.1
PbSe	0.165	3.0	66.12	4.94;0.87	14.08;2.83	87.58	4.8
PbTe	0.190	2.2	66.80	5.86;1.46	12.12;2.01	186.90	5.6

4.2. Ravindra Relation

As Ravindra relation is a linear relation, it is produced by expanding Equation (33) and approximating it by just taking into account the linear parts. This results,

$$n = \sqrt{K_o} - \frac{\sqrt{K_o}}{2K} E_g \quad (38)$$

The similar linear relationship was derived by Gupta and Ravindra [12], who found that the values of $\sqrt{K_o}$ (≈ 4.084) and $\frac{\sqrt{K_o}}{2K}$ (≈ 0.62) by empirical fittings. Table 1 highlights the calculated values of K_1 and K_2 for different materials.

4.3. Herve-Vandamme Relation

Herve and Vandamme made the assumption that $K = B$, or the constant difference of " $E_o - E_g$ " had a B parameter with a value of 3.4 eV. Replacing K with B and performing a simple computation of Equation (33) yields,

$$n^2 = 1 + \frac{E_d E_o}{(E_g + B)^2} \quad (39)$$

This shows that $A = \sqrt{E_d E_o}$. Conversely, beginning with $E_d E_o = A^2$ produces the expression,

$$(K + E_g)^2 \left[\frac{K_o K}{K + E_g} - 1 \right] = A^2 \quad (40)$$

This eventually leads to,

$$K_o \left[1 + \frac{E_g}{K} \right]^{-1} = 1 + \frac{A^2}{(E_g + B)^2} \quad (41)$$

Using empirical fitting of experimental data, they computed A to be 13.6 eV and regarded it as the ionization energy of a Hydrogen atom. Table 1 highlights the calculated values of A and B for different materials.

5. Discussion

5.1. Empirical fitting constants

So far, it has been shown that the empirical fitting constants associated with the Moss, Ravindra, and Herve-Vandamme relationships are connected to K_o and K , which are functions of E_o and E_d . These constants are thus specific to each material, and their numerical values were previously determined through empirical fitting. Table 1 highlights the computed values of these constants for different materials. Originally, the Ravindra constants K_1 and K_2 were estimated to be 4.084 and 0.62 eV⁻¹, respectively. Moss utilized the same original value of K_2 as 0.62 eV⁻¹ and computed K to be 6.6 eV, which is quite unrealistic, and so proposed new values of K_1 and K_2 of 3.9 and 1.02 eV⁻¹, respectively [21]. In contrast to Moss, this study (Equation 38) calculates K_o to be 16.68 and K to be 3.29 eV using the same original constants K_1 and K_2 . Later on Ravindra et. al. [22] proposed more updated values of K_1 and K_2 to be 4.16 and 0.85 eV⁻¹. With the help of Ravindra two constants, the single Moss constant can also be predicted using Equation 37. The predicted values of Moss constant using original K_1 and K_2 is 183.24 eV, Moss estimated K_1 and K_2 is 88.42 eV and Ravindra later updated values of K_1 and K_2 is 146.47 eV. The Herve-Vandamme relation can also be used to predict the lowest bound of the Moss constant. As $K_o^2 K = \frac{(E_d + E_o)^2}{K}$ and so $K_o^2 K = \frac{4(\frac{E_d + E_o}{2})^2}{K}$. Since $\frac{E_d + E_o}{2} \geq \sqrt{E_d E_o}$; this implies $K_o^2 K \geq \frac{4E_d E_o}{K}$. Figure 1 shows the values of refractive indices of various materials calculated using Moss, Ravindra, and Herve-Vandamme relationships as well as with Equation 33, and compared with their respective experimental values.

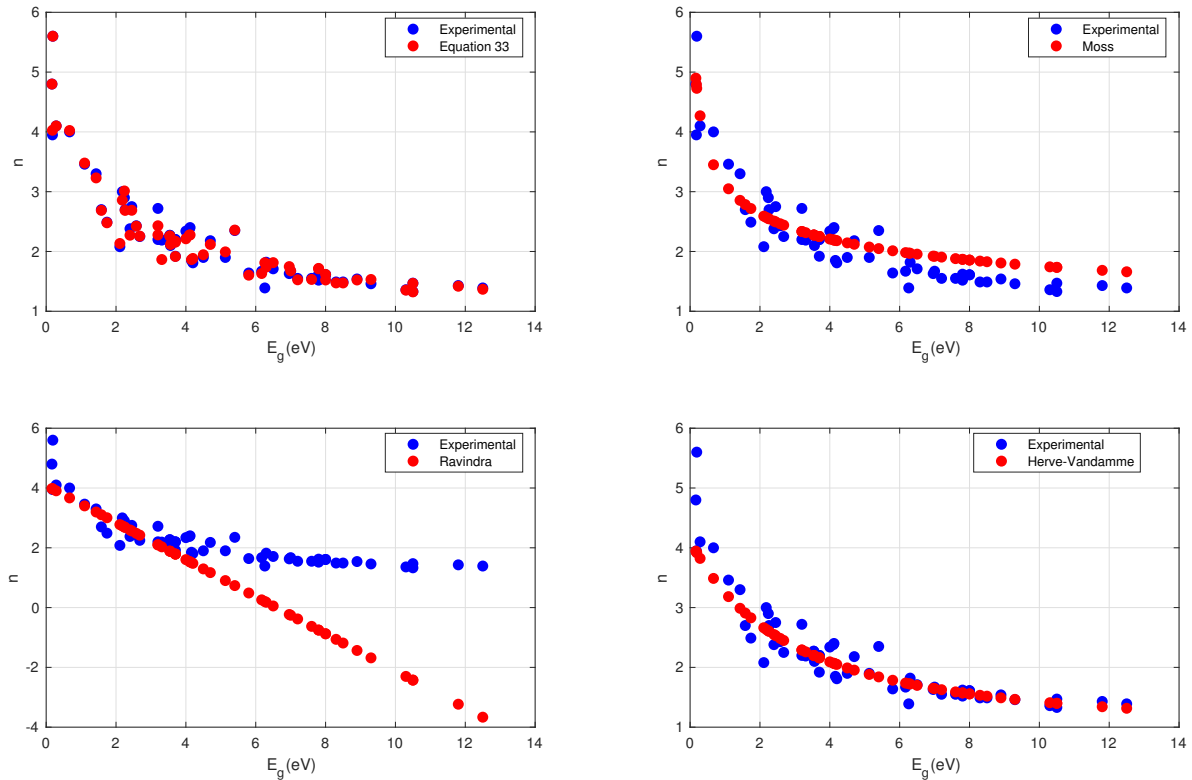


Figure 1. Calculated refractive indices in comparison to experimental values .

According to Moss, the relationship between refractive index and energy gap must be the result of a close relationship between the energy gap and the UV absorption peak, with $K = E_o - E_g$ being one of the simplest assumptions [21]. This notion is directly used in the Herve-Vandamme relation, which assumes that the difference between the UV resonance energy and the energy gap is constant and assigns it a value of 3.4 eV [16], whereas Ravindra relation implicitly assigns it a value of 3.29 eV . Unlike the Moss relation, the presence of two constants in Ravindra and Herve-Vandamme relations is most likely due to one of the constants explicitly or implicitly representing this constant difference. Moreover, this study also demonstrates that the WD model directly leads to this simplest assumption of $K = E_o - E_g$, which is sufficient to integrate the Moss, Ravindra, and Herve-Vandamme relations. However, the true nature of the refractive index dependence between the energy gap and oscillator resonance energy remains hidden. In other words, the WD model directly leads us to assume p as unity, but whether $p = 1$ is true value or not is still unknown.

5.2. Convergence criterion

The convergence criteria that leads to Equation 33 is $|\frac{E_g}{K}| < 1$. In order to satisfy the requirement $|\frac{E_g}{K}| < 1$, E_o must be more than twice that of E_g ($E_o > 2E_g$), which in turn satisfy the requirement $K > E_g$. Based on this criteria, one can claim that the Ravindra relation should deviate when $E_g > 3.29 \text{ eV}$ and Herve-Vandamme relation should deviate when $E_g > 3.4 \text{ eV}$. This claim is somehow true for Ravindra relation but not true for Herve-Vandamme relation. Similarly for Moss relation, it appears that the denominator of the right hand term in Equation 34 is quite independent of the condition $|\frac{E_g}{K}| < 1$. Because if $|\frac{E_g}{K}| < 1$ then $|\frac{K}{E_g}| > 1$, and if $|\frac{E_g}{K}| > 1$ then $|\frac{K}{E_g}| < 1$, leaving the term $(2 + \frac{E_g}{K} + \frac{K}{E_g})$ unchanged, resulting the Moss constant independent of the condition. Moreover, there are materials such as KF , $NaCl$, $NaBr$ (one can find from Table 1) where the convergence criteria $|\frac{E_g}{K}| < 1$ is violated but the indices predicted by Equation 33 is close to their respective experimental values. This contradiction implies that n should fall exponentially on $|\frac{E_g}{K}|$ until the ratio reaches unity,

and then n should be roughly constant with $|\frac{E_g}{K}|$. This means that for two or more materials having similar E_d and $|\frac{E_g}{K}| > 1$ have similar refractive indices. As a result, the variation of n with E_g should be of an exponentially decreasing character, with asymptotes at $n = 1$.

5.3. Exceptional materials

Moss stated in his work [21] that materials such as *Ge*, *InSb*, and *PbS* have almost the same indices despite vastly different energy gaps. Moss, Ravindra, and Herve-Vandamme relationships also vary significantly in IV-VI materials such as *PbS*, *PbSe*, and *PbTe* despite these materials satisfy $|\frac{E_g}{K}| < 1$ [9,16,21]. These remarkable materials are infrared materials, and the unique constant/constants generated by empirical fitting of distinct materials diverge substantially for such low gap materials. As previously demonstrated, the constants are a function of E_o and E_d , and the variation in the refractive index is due to the combined action of E_g or E_o , and E_d . The refractive indices of these materials are shown in Table 2 and are well predicted by Equation 33.

Table 2. Computed values of refractive indices of different materials.

	$E_g(eV)$	Moss (n)	Ravindra (n)	$H - V$ (n)	Equation 33 (n)	$n(exp)$
<i>Ge</i>	0.67	3.45	3.66	3.48	4.02	4.0
<i>InSb</i>	0.18	4.79	3.97	3.93	4.02	3.95
<i>PbS</i>	0.286	4.27	3.90	3.94	4.09	4.1
<i>PbSe</i>	0.165	4.89	3.98	3.94	4.79	4.8
<i>PbTe</i>	0.190	4.73	3.96	3.92	5.51	5.6

6. Conclusions

In conclusion, using the WD model, this paper formulates an accurate equation relating $n-E_g$ as $n^2 = K_o \left[1 + \frac{E_g}{K}\right]^{-1}$, where K_o and K can be found for each material based on their respective E_o and E_d . It has been demonstrated that this equation can accurately describe all types of materials (from low energy gaps to high energy gaps). Furthermore, this formulation is enough for integrating the Moss, Ravindra, and Herve-Vandamme relations and comprehending their empirical fitting constants.

Funding: The author declare that they have no known competing financial interests or personal relationships that could have appeared to influence the work reported in this paper.

Data Availability Statement: The data presented in this study are available on request from the corresponding author.

Acknowledgments: I would like to remember Prof. N.M. Ravindra of New Jersey Institute of Technology, for his outstanding work and contributions in the field of semiconductors. I have had the opportunity to work with him during my Ph.D. This paper is dedicated to him.

Conflicts of Interest: The author declare no conflict of interest.

References

1. Ou, Q.; Bao, X.; Zhang, Y.; Shao, H.; Xing, G.; Li, X.; Shao, L.; Bao, Q. Band structure engineering in metal halide perovskite nanostructures for optoelectronic applications. *Nano Materials Science* **2019**, *1*, 268–287.
2. Geng, T.; Ma, Z.; Chen, Y.; Cao, Y.; Lv, P.; Li, N.; Xiao, G. Bandgap engineering in two-dimensional halide perovskite Cs₃Sb₂I₉ nanocrystals under pressure. *Nanoscale* **2020**, *12*, 1425–1431.
3. Wu, M.J.; Kuo, C.C.; Jhuang, L.S.; Chen, P.H.; Lai, Y.F.; Chen, F.C. Bandgap engineering enhances the performance of mixed-cation perovskite materials for indoor photovoltaic applications. *Advanced Energy Materials* **2019**, *9*, 1901863.

4. Nenkov, M.R.; Pencheva, T.G. Determination of thin film refractive index and thickness by means of film phase thickness. *Central European Journal of Physics* **2008**, *6*, 332–343.
5. Ono, M.; Aoyama, S.; Fujinami, M.; Ito, S. Significant suppression of Rayleigh scattering loss in silica glass formed by the compression of its melted phase. *Optics Express* **2018**, *26*, 7942–7948.
6. Ong, H.; Dai, J.; Li, A.; Du, G.; Chang, R.; Ho, S. Effect of a microstructure on the formation of self-assembled laser cavities in polycrystalline ZnO. *Journal of Applied Physics* **2001**, *90*, 1663–1665.
7. Moss, T.S. A Relationship between the Refractive Index and the Infra-Red Threshold of Sensitivity for Photoconductors. *Proceedings of the Physical Society. Section B* **1950**, *63*, 167. doi:10.1088/0370-1301/63/3/302.
8. Moss, T.S. Photoconductivity in the Elements. *Proceedings of the Physical Society. Section A* **1951**, *64*, 590.
9. Ravindra, N.; Srivastava, V. Variation of refractive index with energy gap in semiconductors. *Infrared Physics* **1979**, *19*, 603–604. doi:10.1016/0020-0891(79)90081-2.
10. Reddy, R.; Nazeer Ahammed, Y. A study on the Moss relation. *Infrared Physics & Technology* **1995**, *36*, 825–830. doi:https://doi.org/10.1016/1350-4495(95)00008-M.
11. Ravindra, N.; Auluck, S.; Srivastava, V. On the Penn Gap in Semiconductors. *physica status solidi (b)* **1979**, *93*, K155–K160. doi:10.1002/pssb.2220930257.
12. Gupta, V.; Ravindra, N. Comments on the Moss Formula. *physica status solidi (b)* **1980**, *100*, 715–719. doi:10.1002/pssb.2221000240.
13. Penn, D.R. Wave-Number-Dependent Dielectric Function of Semiconductors. *Phys. Rev.* **1962**, *128*, 2093–2097. doi:10.1103/PhysRev.128.2093.
14. Wemple, S.; DiDomenico Jr, M. Behavior of the electronic dielectric constant in covalent and ionic materials. *Physical Review B* **1971**, *3*, 1338.
15. Wemple, S.H.; DiDomenico, M. Optical Dispersion and the Structure of Solids. *Phys. Rev. Lett.* **1969**, *23*, 1156–1160. doi:10.1103/PhysRevLett.23.1156.
16. Hervé, P.; Vandamme, L. General relation between refractive index and energy gap in semiconductors. *Infrared physics & technology* **1994**, *35*, 609–615.
17. Finkenrath, H. The Moss rule and the influence of doping on the optical dielectric constant of semiconductors—I. *Infrared Physics* **1988**, *28*, 327–332. doi:https://doi.org/10.1016/0020-0891(88)90054-1.
18. Sellmeier. Zur Erklärung der abnormen Farbenfolge im Spectrum einiger Substanzen. *Annalen der Physik*, *219*, 272–282.
19. Levi, A.F.J. The Lorentz oscillator model. In *Essential Classical Mechanics for Device Physics*; 2053–2571, Morgan & Claypool Publishers, 2016; pp. 5–1 to 5–21. doi:10.1088/978-1-6817-4413-1ch5.
20. Gomaa, H.M.; Yahia, I.; Zahran, H. Correlation between the static refractive index and the optical bandgap: Review and new empirical approach. *Physica B: Condensed Matter* **2021**, *620*, 413246. doi:https://doi.org/10.1016/j.physb.2021.413246.
21. Moss, T.S. Relations between the Refractive Index and Energy Gap of Semiconductors. *physica status solidi (b)* **1985**, *131*, 415–427, [https://onlinelibrary.wiley.com/doi/pdf/10.1002/pssb.2221310202]. doi:https://doi.org/10.1002/pssb.2221310202.
22. Ravindra, N.; Ganapathy, P.; Choi, J. Energy gap–refractive index relations in semiconductors – An overview. *Infrared Physics & Technology* **2007**, *50*, 21–29. doi:https://doi.org/10.1016/j.infrared.2006.04.001.

Disclaimer/Publisher's Note: The statements, opinions and data contained in all publications are solely those of the individual author(s) and contributor(s) and not of MDPI and/or the editor(s). MDPI and/or the editor(s) disclaim responsibility for any injury to people or property resulting from any ideas, methods, instructions or products referred to in the content.